The EMBO Journal (2012) 31, 1177–1189 | © 2012 European Molecular Biology Organization | All Rights Reserved 0261-4189/12
www.embojournal.org

THE EMBO JOURNAL

ATR maintains select progenitors during nervous system development

Youngsoo Lee[1,5], Erin RP Shull[1,2,5], Pierre-Olivier Frappart[1,3,5], Sachin Katyal[1], Vanessa Enriquez-Rios[1,2], Jingfeng Zhao[1], Helen R Russell[1], Eric J Brown[4] and Peter J McKinnon[1,2,*]

[1]Department of Genetics, St Jude Children's Research Hospital, Memphis, TN, USA; [2]Graduate Health Sciences, University of Tennessee, Memphis, TN, USA; [3]DKFZ, Heidelberg, Germany and [4]Department of Cancer Biology, Abramson Family Cancer Research Institute, Philadelphia, PA, USA

The ATR (ATM (ataxia telangiectasia mutated) and rad3-related) checkpoint kinase is considered critical for signalling DNA replication stress and its dysfunction can lead to the neurodevelopmental disorder, ATR-Seckel syndrome. To understand how ATR functions during neurogenesis, we conditionally deleted *Atr* broadly throughout the murine nervous system, or in a restricted manner in the dorsal telencephalon. Unexpectedly, in both scenarios, Atr loss impacted neurogenesis relatively late during neural development involving only certain progenitor populations. Whereas the Atr-deficient embryonic cerebellar external germinal layer underwent p53- (and $p16^{Ink4a/Arf}$)-independent proliferation arrest, other brain regions suffered apoptosis that was partially p53 dependent. In contrast to other organs, in the nervous system, p53 loss did not worsen the outcome of *Atr* inactivation. Coincident inactivation of *Atm* also did not affect the phenotype after *Atr* deletion, supporting non-overlapping physiological roles for these related DNA damage-response kinases in the brain. Rather than an essential general role in preventing replication stress, our data indicate that ATR functions to monitor genomic integrity in a selective spatiotemporal manner during neurogenesis.

The EMBO Journal (2012) **31,** 1177–1189. doi:10.1038/emboj.2011.493; Published online 20 January 2012
Subject Categories: genome stability & dynamics; molecular biology of disease
Keywords: ATM; ATR; DNA damage; neural development; Seckel syndrome

Introduction

Maintenance of DNA integrity during development is achieved by signalling pathways that respond to DNA damage to pause cell proliferation and allow DNA repair, or alternatively, activate apoptosis and eliminate cells to avoid the potential acquisition of mutations (Jackson and Bartek, 2009). Many human DNA repair-deficiency syndromes are characterized by pronounced congenital neuropathology, including neurodevelopmental disease that result from faulty signalling associated with replication stress (McKinnon, 2009). During neurogenesis, the rapid expansion of neural tissue makes replication-associated DNA damage a particular problem, which is circumvented by signalling pathways that efficiently respond to replication-associated DNA damage (Branzei and Foiani, 2010; Lopez-Contreras and Fernandez-Capetillo, 2010).

ATR (ataxia telangiectasia and rad3-related) is an essential protein kinase that prevents DNA damage accumulation during replication, and mutation of this kinase can result in the developmental disorder, ATR-Seckel syndrome (O'Driscoll *et al*, 2003). ATR is critical during S-phase and responds to stalled replication forks by activation of cell-cycle arrest via phosphorylation of Chk1 and the modulation of fork repair factors (Liu *et al*, 2000; Zhao and Piwnica-Worms, 2001; Rouse, 2004; Ohouo *et al*, 2010; Nam and Cortez, 2011). This kinase also broadly responds to ancillary DNA damage that can perturb replication such as UV-induced pyrimidine dimers or base adducts (Cimprich and Cortez, 2008; Shiotani and Zou, 2009a). ATR is specifically activated by replication protein A (RPA)-coated stretches of single-strand DNA (ssDNA) that accumulate at stalled replication forks or during homologous recombination repair (Zou and Elledge, 2003; Cimprich and Cortez, 2008; Shiotani and Zou, 2009a). The ATR-interacting protein (ATRIP) is an essential co-factor for ATR activity and is required for directly targeting ATR to RPA-coated ssDNA (Cortez *et al*, 2001; Zou and Elledge, 2003; Xu *et al*, 2008). ATR signalling further depends on the RAD9–RAD1–HUS1 (9–1–1) complex that recognizes a DNA end adjacent to RPA-bound ssDNA that facilitates localization of the ATR activator, TopBP1 to the ATR/ATRIP complex (Kumagai *et al*, 2006; Delacroix *et al*, 2007; Lee *et al*, 2007; Sohn and Cho, 2009). TopBP1 is critical for ATR activation, and the ability of ATRIP to directly bind TopBP1 likely facilitates this process (Kumagai *et al*, 2006; Mordes *et al*, 2008). Additionally, the chromatin-associated factor Claspin also associates with ATR in a damage-dependent manner and is required for the activation and checkpoint function of ATR (Chini and Chen, 2003; Kumagai and Dunphy, 2003; Lee *et al*, 2003; Sar *et al*, 2004). Finally, many additional ATR protein substrates have been identified, although the link to ATR function in most cases is unclear (Matsuoka *et al*, 2007).

An ATR-related DNA damage-activated kinase, ATM (ataxia telangiectasia mutated) is also critical for the DNA damage response (DDR) and its inactivation leads to the neurodegenerative disease, ataxia telangiectasia (Chun and Gatti, 2004; Shiloh, 2006; Lavin, 2008; McKinnon, 2012). In contrast to ATR, ATM is activated via the MRN (Mre11/Rad50/Nbs1) complex, which functions as a DNA damage sensor to detect

*Corresponding author. Department of Genetics, St Jude Children's Research Hospital, Memphis, TN 38105, USA. Tel.: +1 901 595 2700; Fax: +1 901 595 6035; E-mail: peter.mckinnon@stjude.org
[5]These authors contributed equally to this work

Received: 22 July 2011; accepted: 19 December 2011; published online: 20 January 2012

and tether DNA double-strand breaks (Hopfner *et al*, 2002; Stracker *et al*, 2004; Moreno-Herrero *et al*, 2005). ATM and ATR can phosphorylate many of the same substrates in response to DNA damage (Matsuoka *et al*, 2007). In part, this may reflect that sequential processing of DNA damage during repair can generate intermediates that activate either kinase (Cimprich and Cortez, 2008; Tomimatsu *et al*, 2009; Shiotani and Zou, 2009b). However, the interrelationship between ATM and ATR during the DDR is not entirely clear. Increasingly, evidence for a direct cooperation between these kinases suggests that modulation of ATR function can occur directly or indirectly by ATM kinase activity (Jazayeri *et al*, 2006; Cuadrado *et al*, 2006b; Yoo *et al*, 2007, 2009; Limbo *et al*, 2011).

While cellular studies have been instrumental in determining the biochemistry of the DDR and checkpoint integration, a challenge remains in understanding these responses in a physiological context. ATR has been shown to prevent replicative stress *in utero*, which results in perturbation of tissue homeostasis or regeneration, and it is also required for adult hippocampal neurogenesis (de Klein *et al*, 2000; Ruzankina *et al*, 2007, 2009; Murga *et al*, 2009; Onksen *et al*, 2011). Further, recent studies indicate that p53 loss substantially exacerbated these phenotypes following Atr disruption (Murga *et al*, 2009; Ruzankina *et al*, 2009). Here, we have addressed the specific role of Atr within the nervous system and found that rather than a broad requirement during neurogenesis, Atr is important for maintaining select neural progenitor cells. Moreover, while Atr dysfunction resulted in perturbed neurogenesis and growth defects, this was independent of p53 or Atm signalling. Our data uncover novel ATR-dependent strategies that maintain genome integrity during development.

Results

Atr loss results in growth defects and cerebellar dysgenesis

ATR is a key signal transducer of replication stress, and while it is critical for normal cell-cycle progression *in vitro*, its specific physiological functions are less clear. Therefore, we determined the requirement for ATR during neurogenesis using *Nestin-cre* to inactivate mouse *Atr* throughout the nervous system. In contrast to germline inactivation that results in lethality around E6.5 (Brown and Baltimore, 2000; de Klein *et al*, 2000), $Atr^{LoxP/LoxP}$; *Nestin-cre* (hereafter, $Atr^{Nes\text{-}cre}$), mice were viable but showed growth retardation, reduced brain and body size and marked defects in cerebellar development (Figure 1A; Supplementary Figure S1) and died around postnatal day 7 (P7). *Nestin-cre* drives gene deletion throughout the nervous system beginning at embryonic day 10.5 (E10.5) and highly efficient *Atr* deletion and protein loss occurred in the $Atr^{Nes\text{-}cre}$ brain (Figure 1B and C).

Histological analysis of $Atr^{Nes\text{-}cre}$ mice revealed many abnormalities including decreased cellularity in the cerebral cortex (CTX) and the corpus callosum (CC), and in the olfactory bulb the granule cell layer was depleted (Figure 1D). The severe effects in the $Atr^{Nes\text{-}cre}$ cerebellum are due to granule neuron loss leading to defective foliation and mislocalization of calbindin-positive Purkinje cells (Figure 1A and E). To account for these phenotypes, we determined the developmental impact of Atr loss during neurogenesis.

DNA damage is restricted to specific $Atr^{Nes\text{-}cre}$ progenitor cell populations

Given the role of ATR in preventing replication-associated DNA damage, we surveyed the $Atr^{Nes\text{-}cre}$ embryonic central nervous system for DNA damage using γH2AX immunostaining. Coincident with defective cerebellar development, we found γH2AX immunoreactivity in the $Atr^{Nes\text{-}cre}$ cerebellar external granule layer (EGL) from E15.5 (Figure 2A). γH2AX-positive cells were localized to the proliferative EGL and rhombic lip (RL), while other regions of the $Atr^{Nes\text{-}cre}$ embryonic cerebellum such as the ventricular zone (VZ) showed few cells marked by DNA damage, despite being a site of abundant proliferation (Supplementary Figure S2). Although apoptosis was not elevated at E15.5, by E16.5 the EGL contained occasional apoptotic cells as determined using TUNEL labelling (Figure 2B). The TUNEL staining coincided with phosphorylated p53ser18 (Figure 2B), which is characteristic of DNA damage in this tissue (Lee and McKinnon, 2007).

In contrast to the cerebellum, the ganglionic eminence (GE), a structure responsible for generating a diversity of cortical cell types (Lavdas *et al*, 1999; Corbin *et al*, 2001; Molyneaux *et al*, 2007; Rudy *et al*, 2011), exhibited high levels of DNA damage (γH2AX immunostaining) at E15.5 after Atr loss. Further, abundant apoptosis, as determined by active caspase-3 and TUNEL staining, was also present in the $Atr^{Nes\text{-}cre}$ GE (Figure 2C), but not elsewhere through the forebrain or hindbrain (Figure 2D). However, apart from the GE and EGL, minimal γH2AX immunostaining or cell death was observed elsewhere in the nervous system at this developmental stage. Therefore, through mid-gestation, Atr is essential in a restricted spatiotemporal manner for neural development.

Atr loss leads to proliferation defects in cerebellar EGL progenitors

While apoptosis was robust in the GE at E15.5, the overall levels of cell death observed in the embryonic cerebellum were relatively low and appeared insufficient to account for the pronounced developmental defects in the $Atr^{Nes\text{-}cre}$ cerebellum (Figure 1A and E). We therefore determined if cell-cycle arrest, an alternate outcome to apoptosis after DNA damage, contributed to perturbed cerebellar development in $Atr^{Nes\text{-}cre}$ mice. We found normal indices of proliferation throughout the cerebellum at E15.5 using PCNA and BrdU (5-bromo-2′-deoxyuridine) immunolabelling at E15.5 (Figure 3A). However, by E16.5, there was a striking defect in the proliferating EGL (Figure 3). We found an 80% reduction in proliferation within the $Atr^{Nes\text{-}cre}$ cerebellar EGL and RL compared with control tissue as determined using PCNA or BrdU immunolabelling (Figure 3C). This proliferation defect in the EGL and the consequent failure to generate granule neuron progenitors (GNPs) is consistent with the cerebellar dysgenesis observed postnatally (Figure 3D). In comparison to proliferation defects, we found little apoptosis in the mutant embryonic cerebellum between E15.5–17.5.

In striking contrast to the EGL, the VZ of the $Atr^{Nes\text{-}cre}$ cerebellum, which produces multiple cerebellar cell types including interneurons and Purkinje cells, showed normal proliferation compared with controls at E17.5 (Figure 3C). We also used SOX2 immunolabelling to further confirm that the effect of Atr loss was confined to the EGL. SOX2 is a transcription factor required for maintenance of neural stem/progenitor

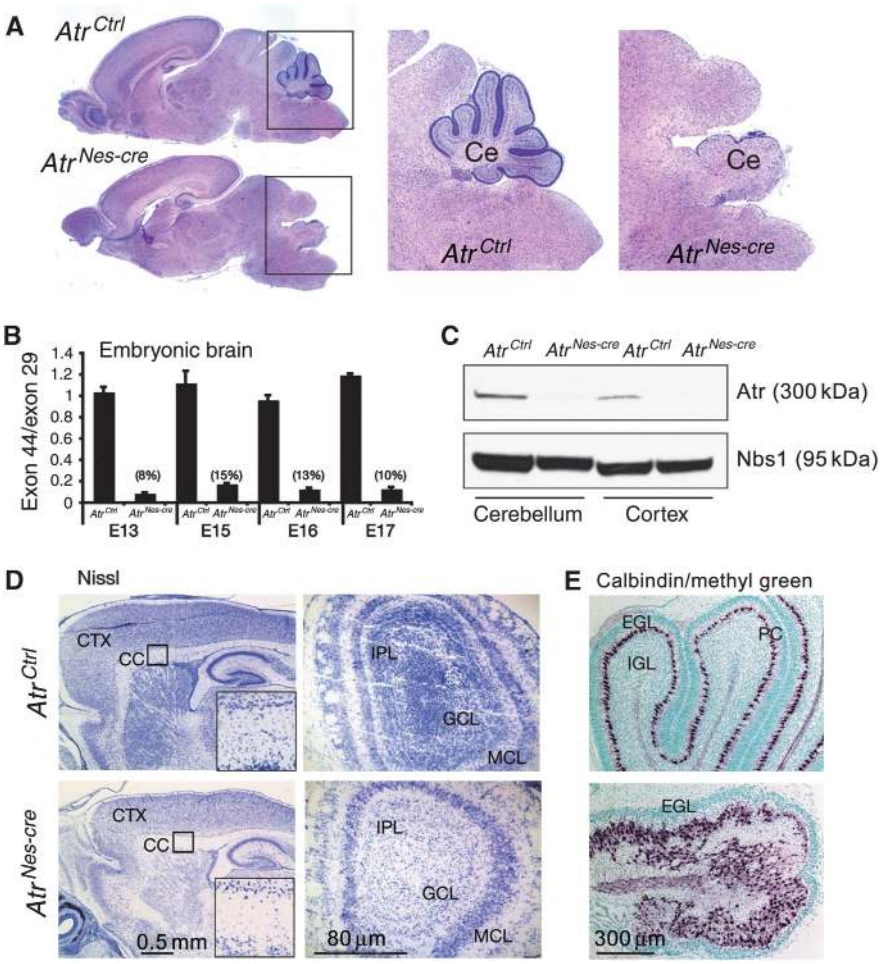

Figure 1 Atr loss leads to defective neurogenesis. (**A**) Atr loss results in microcephaly and defective cerebellar development. Haematoxylin and eosin staining of Atr^{Ctrl}, $Atr^{Nes\text{-}cre}$ brain sections at P6 reveals a dramatic reduction of the mutant cerebellum compared with WT, indicating that the cerebellum is markedly affected compared with other brain regions (mag. ×2.5). Ce, cerebellum. (**B**) Atr gene deletion occurs efficiently by E13.5 as determined using real-time PCR. (**C**) Atr protein is disrupted in P5 cerebellum and cortex; Nbs1 is shown as a control for protein blotting. (**D**) Cellularity of the $Atr^{Nes\text{-}cre}$ brain is reduced, with cortical layer thinning and loss of CC cellularity (enlarged boxed region); shown using Nissl staining of the cortex and olfactory bulb, respectively. (**E**) Disruption of the Purkinje cell layer in the $Atr^{Nes\text{-}cre}$ cerebellum is indicated using calbindin immunostaining. PC, Purkinje cells; EGL, external granular layer; IGL, inner granule layer; IPL, internal plexiform layer; GCL, granule cell layer; MCL, mitral cell layer.

cells, and in the cerebellum it is expressed exclusively in the RL and VZ (Zappone *et al*, 2000; Suh *et al*, 2007). The total number of SOX2-positive cells in the $Atr^{Nes\text{-}cre}$ cerebellar VZ was similar between control and $Atr^{Nes\text{-}cre}$ tissue at E16.5 (Supplementary Figure S3). These data highlight the essential selective requirement for ATR during proliferation of the GNPs.

Atr inactivation in the dorsal telencephalon leads to moderate cortical hypoplasia

Although the cerebellum and GE were markedly affected in $Atr^{Nes\text{-}cre}$ animals, the effect of Atr inactivation towards neural development elsewhere was surprisingly mild. In fact, it was notable that Atr was relatively dispensable through mid-gestational development. We therefore considered if the timing of *Atr* deletion influences the phenotype, such that early progenitors might manifest a greater effect of Atr loss. To address this, we used *Emx1-cre* to direct *Atr* deletion in the early dorsal telencephalic progenitors in the neopallial cortex (Gorski *et al*, 2002). This approach targets progenitors that give rise to the cortex and facilitates gene inactivation around one day earlier than *Nestin-cre*-mediated deletion occurs in these cells (Chou *et al*, 2009).

We generated $Atr^{Emx1\text{-}cre}$ mice and found only a moderate perturbation of cortical development, despite effective inactivation of Atr (Figure 4A and C). However, the hippocampal formation, which derives from Emx1-progenitors, was clearly affected and showed reduced cellularity, indicating efficient *Emx1-cre*-mediated Atr deletion (Figure 4A). This contrasts the situation when the ATR activator, TopBP1, is deleted via a similar strategy as extensive cortical ablation occurs in $TopBP1^{Emx1\text{-}cre}$ mice, indicating that TopBP1 is essential in Emx1-progenitors (Figure 4B). These data indicate that Atr function is dispensable for cortical progenitor proliferation.

Although overall cortical development occurred in the $Atr^{Emx1\text{-}cre}$ brain, there was nonetheless an obvious reduction in cortical size (Figure 4A and E). This resulted from apoptosis, as analysis showed widespread areas of the neopallium was γH2AX and TUNEL positive with an associated reduction in proliferation as determined using BrdU and phospho-H3

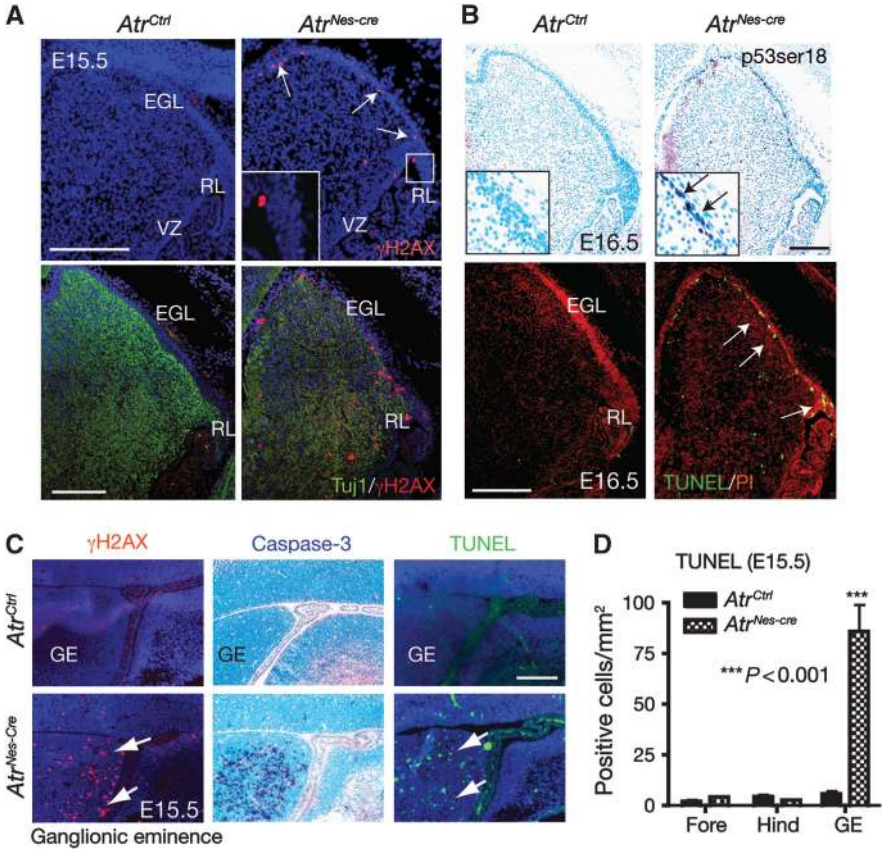

Figure 2 Atr deficiency leads to DNA damage accumulation and increased apoptosis in neural progenitors. (**A**) Loss of Atr leads to increased DNA damage at E15.5 indicated by H2AX phosphorylation (γH2AX). Tuj1 immunostaining identifies immature cerebellar neurons. Arrows indicate γH2AX signal. (**B**) p53 protein and apoptosis (arrows) are increased in the E16.5 $Atr^{Nes\text{-}cre}$ EGL. (**C**) The $Atr^{Nes\text{-}cre}$ medial GE at E15.5 shows increased DNA damage (γH2AX), caspase-3 activation and apoptosis (TUNEL staining). (**D**) Quantification of apoptotic cells in various $Atr^{Nes\text{-}cre}$ brain regions shows that the GE is markedly affected by Atr loss.

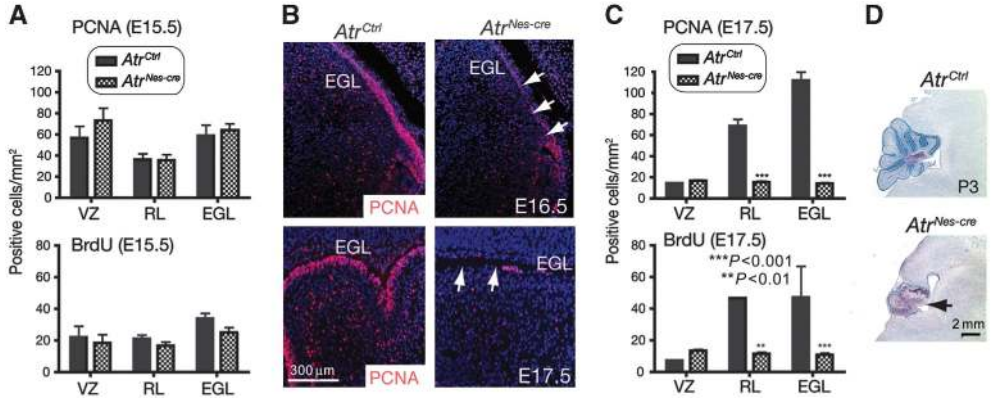

Figure 3 Granule neuron precursor proliferation is decreased in the $Atr^{Nes\text{-}cre}$ cerebellum. (**A**) At E15.5, the numbers of PCNA and BrdU positive proliferating precursors are similar in all cerebellar germinal zones; the VZ, the RL and the EGL. (**B**) In comparison, there is a marked reduction of PCNA-positive precursors from E16.5 to E17.5. (**C**) At E17.5, quantitative analysis shows the reduction in proliferation in the $Atr^{Nes\text{-}cre}$ EGL and RL, but not in the VZ. (**D**) The postnatal $Atr^{Nes\text{-}cre}$ cerebellum (indicated by arrow) lacks an EGL with granule neuron precursors that results in an unordered Purkinje cell layer. Purkinje cells are identified using calbindin immunostaining.

immunostaining (Figure 4D). To more carefully judge the overall impact of Atr loss on cortical development, we assessed cortical layer organization. Although all layers were readily identifiable by layer-specific immunostaining, we found reduced cellularity and less demarcation, particularly in layers IV–II (Figure 4E). For example, there was a paucity of cells revealed by Cux1 immunostaining in upper layers II–III of the $Atr^{Emx1\text{-}cre}$ cortex. Cells immunostaining for Ctip2, which mark layer V, were also reduced. There was also less layer definition indicated by diffuse Foxp1 and Tbr1 staining,

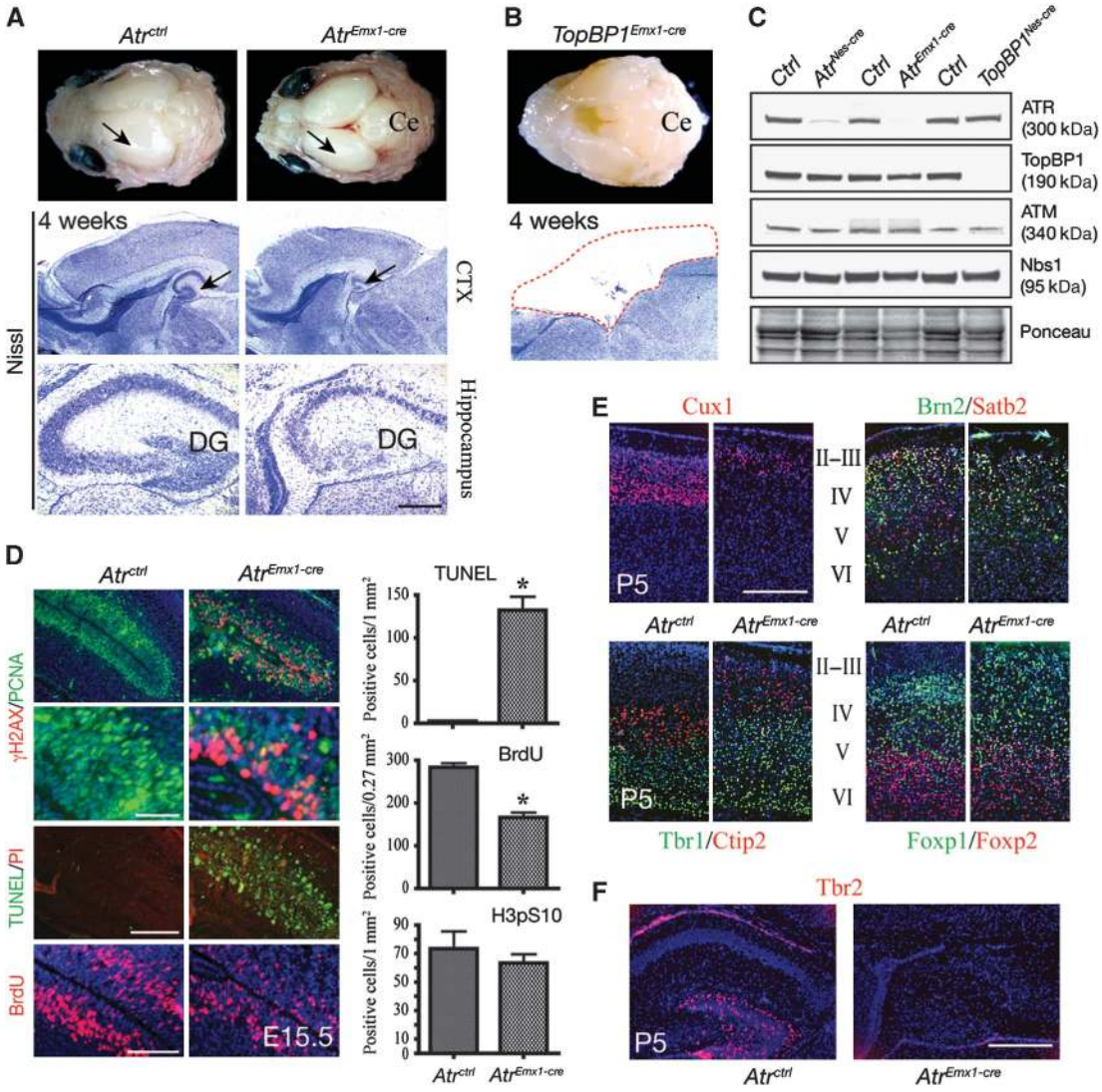

Figure 4 Effect of Atr loss in the dorsal telencephalon. (**A**) Inactivation of Atr in the dorsal telencephalic progenitors in $Atr^{Emx1\text{-}cre}$ mice shows a modest effect towards cortical development, while there is a pronounced loss of hippocampal cellularity (arrows). Ce, cerebellum; DG, dentate gyrus. (**B**) Extensive cortical ablation is observed in $TopBP1^{Emx1\text{-}cre}$ mice. (**C**) Western blot analysis shows that Atr is effectively inactivated in both *Nestin-cre* and *Emx1-cre* cortex at E14.5, as is TopBP1 in $TopBP1^{Nes\text{-}cre}$ tissue. Atm, Nbs1 and Ponceau are controls for protein loading. (**D**) DNA damage-associated apoptosis occurs from E15.5 in the developing $Atr^{Emx1\text{-}cre}$ neocortex. Quantitative presentation of numbers of TUNEL, BrdU and H3pS10-positive cells in control and $Atr^{Emx1\text{-}cre}$ are shown. *indicates $P<0.05$. (**E**) Cortical lamination is present in $Atr^{Emx1\text{-}cre}$ mice as indicated using multiple cortical markers: Satb2, Cux1 and Brn2 mark layers II–IV, Tbr1 and Foxp2 mark layers VI–V, Ctip2 marks layers V–IV and Foxp1 identifies V–III. (**F**) The $Atr^{Emx1\text{-}cre}$ hippocampus shows an absence of the Tbr2 marker. All scale bars are ~300 μm (**A**–**E**) and ~1.2 mm (**F**). Panels in (**D**–**F**) were counterstained with DAPI (blue) or PI (red).

which may reflect developmental abnormalities in the corticothalamic and corticocortical projection neurons of layers VI–III (Molyneaux *et al*, 2007; Hisaoka *et al*, 2010). Hippocampal development was also disrupted as indicated by a lack of Tbr2 staining (Figure 4F). This contrasts the situation in the $Atr^{Nes\text{-}cre}$ brain, where ordered cortical development is present, although also with reduced upper layer cellularity as revealed by Cux1 immunostaining (Supplementary Figure S4). Because the upper layer neurons develop later than the lower layers but from the same neuroepithelial progenitors, Atr appears critical for ensuring long-term genome integrity in these progenitors.

Another $Atr^{Emx1\text{-}cre}$ region that was strongly affected was the CC, which was markedly reduced in size and cellularity, as is the situation in ATR-Seckel syndrome (Supplementary Figure S5). Conspicuously, we failed to find DNA damage (γH2AX immunostaining) or gliosis (GFAP staining) postnatally, indicating that Atr loss while affecting cortical development did not result in persistent DNA damage or marked perturbation of neural homeostasis (data not shown).

Atr is dispensable for the DNA double-strand break damage response

To determine how Atr loss affects neural development, we used an *in vitro* approach to interrogate Atr function in primary neural cultures. We initially established primary $Atr^{Nes\text{-}cre}$ cortical astrocyte cultures, but found that these incurred high levels of DNA damage associated with an inability to proliferate (Figure 5A). We also generated $Atr^{Nes\text{-}cre}$ neurospheres and found a striking reduction in both the number of neurospheres

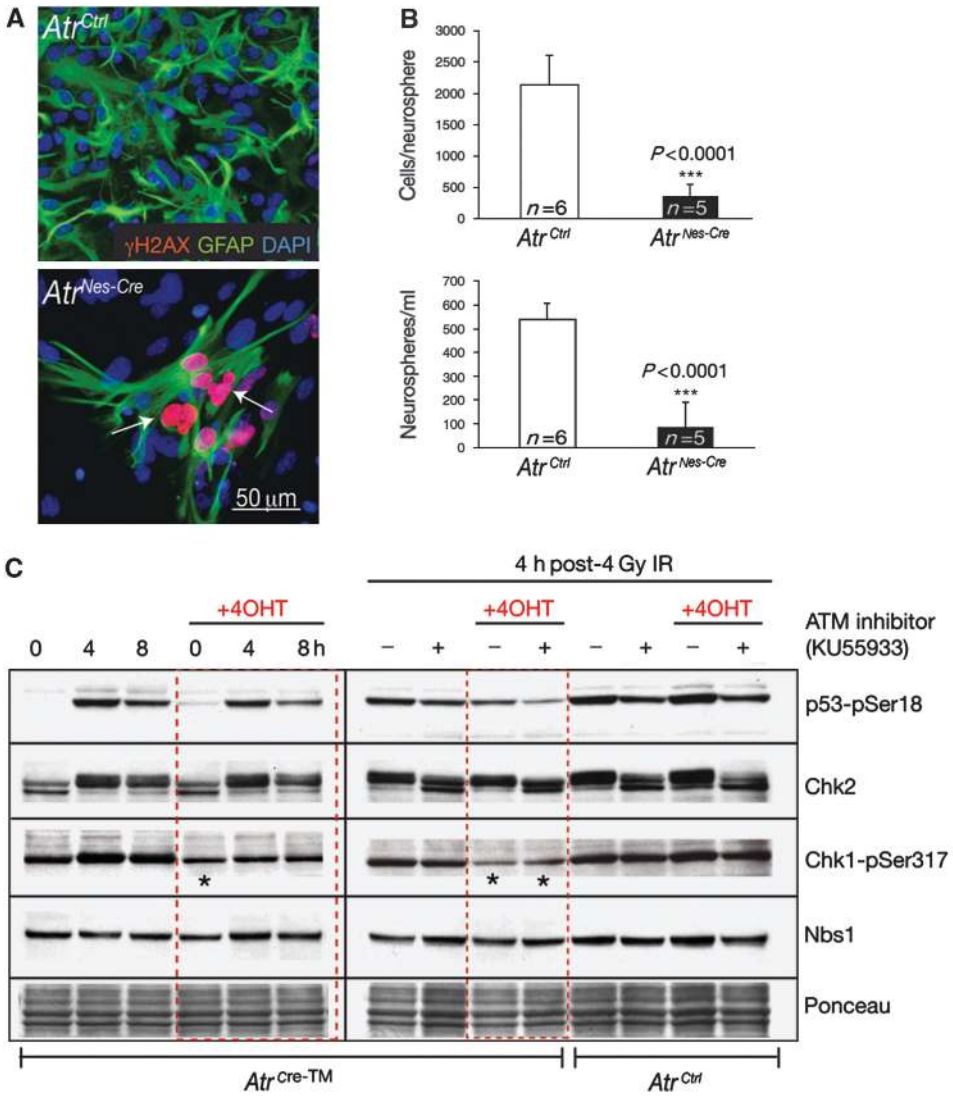

Figure 5 Radiation-induced DNA damage signalling after Atr loss. (**A**) Primary $Atr^{Nes\text{-}cre}$;$p53^{-/-}$ astrocyte cultures accumulated DNA damage (γH2AX; arrows) and failed to proliferate. GFAP is glial fibrillary protein and marks astrocytes. (**B**) $Atr^{Nes\text{-}cre}$ neurospheres also fail to proliferate and are smaller than controls (n = number of individual cultures). (**C**) 4OHT was used to inactivate Atr in $Atr^{Cre\text{-}TM}$ mouse embryonic fibroblasts. After IR, normal Chk2 activation and p53 phosphorylation occurred in Atr-depleted cells. However, phosphorylation of Chk1 was reduced in Atr-depleted cells after IR. Treatment with the ATM inhibitor, KU55933, indicates that the radiation-induced Chk2 shift is Atm dependent. Hatched boxes indicate lanes in which Atr was deleted; Nbs1 was used as a loading control and Ponceau staining shows equal protein transfer.

that we could establish, and a reduced size because of low numbers of cells present in individual neurospheres, again reflecting a proliferation defect (Figure 5B).

To circumvent these issues, we established neurospheres from $Atr^{Cre\text{-}TM}$ animals in which *Atr* deletion could be induced using 4-hydroxy-tamoxifen (4OHT). Atr deletion was efficient after 4OHT administration, and led to smaller neurospheres with decreased proliferation (Supplementary Figure S6A). We assessed the response of $Atr^{Cre\text{-}TM}$ neurospheres after Atr deletion (4OHT treatment) and after exogenous DNA damage using IR. Chk1 phosphorylation was attenuated in $Atr^{Cre\text{-}TM}$ neurospheres, consistent with this being a key Atr substrate (Figure 5C). High basal Chk1 phosphorylation was apparent without 4OHT treatment, but was reduced upon inactivation of Atr (Figure 5C, asterisks), suggesting that neurosphere culture conditions promote replication stress. Irradiation also failed to enhance Chk1 phosphorylation in Atr-deficient neurospheres. However, we found normal Chk2 activation after radiation in the 4OHT-treated $Atr^{Cre\text{-}TM}$ neurospheres, indicating that the early response to DNA DSBs was intact. The relative contribution of Atm and DNA-PK_{CS} during the DDR in $Atr^{Cre\text{-}TM}$ neurospheres was evaluated through acute inhibition of ATM via KU55933 or DNA-PK_{CS} via NU7026. DNA damage-induced Chk2 and p53 activation were attenuated in $Atr^{Cre\text{-}TM}$ neurospheres treated with KU55933, indicating that Atm mediates a DSB response independent of Atr (Figure 5C). In contrast, DNA-PK_{CS} inhibition via NU7026 showed no apparent inhibition of the DDR (Supplementary Figure S6B). We also examined the DDR *in vivo*, in E16.5 $Atr^{Nes\text{-}cre}$ embryos. Similar to *Atr*-deleted neurospheres, we found that radiation-induced Chk2 activation and p53 signalling were normal in $Atr^{Nes\text{-}cre}$ progenitors (Supplementary Figure S7). Thus, while Atr loss leads to a pronounced effect upon cell proliferation, it does

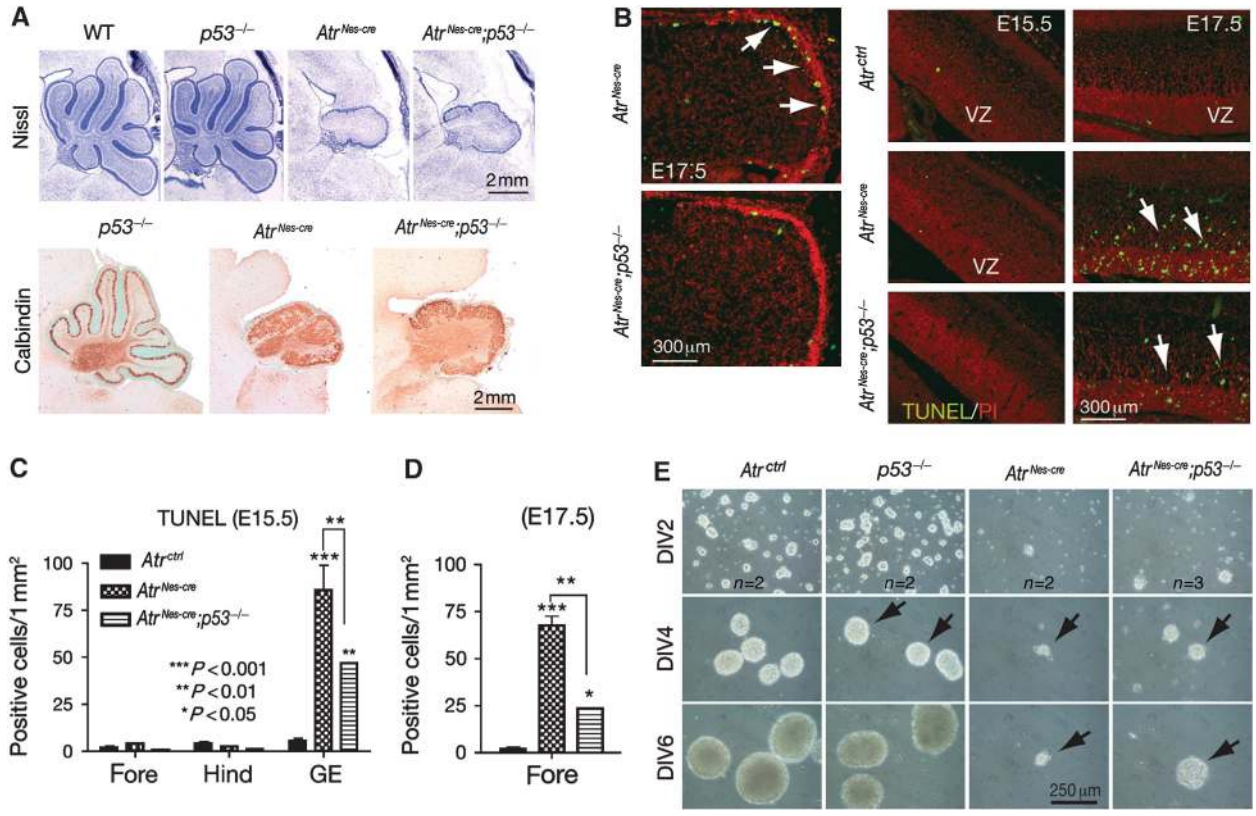

Figure 6 Neurodevelopmental abnormalities in $Atr^{Nes\text{-}cre}$ are not altered by p53 loss. (**A**) The $Atr^{Nes\text{-}cre}$;$p53^{-/-}$ cerebellum is similarly affected to the $Atr^{Nes\text{-}cre}$ brain, indicating that loss of p53 does not affect the cerebellar neurodevelopmental abnormalities. Purkinje cells are identified using calbindin immunostaining. (**B**) While p53 loss fails to abrogate the $Atr^{Nes\text{-}cre}$ phenotype, a portion of the apoptosis in the $Atr^{Nes\text{-}cre}$ GE is p53 dependent. (**C**) Quantification of apoptosis in the $Atr^{Nes\text{-}cre}$ E15.5 forebrain shows apoptosis that is partly p53 dependent. (**D**) TUNEL staining shows that apoptosis in the $Atr^{Nes\text{-}cre}$ cortex is reduced in $Atr^{Nes\text{-}cre}$;$p53^{-/-}$ tissue. (**E**) Neurosphere cultures established from E13.5 embryos of indicated genotypes. DIV, days *in vitro*. Arrows indicate $Atr^{Nes\text{-}cre}$ and $Atr^{Nes\text{-}cre}$;$p53^{-/-}$ neurospheres, *n* is the number of independent neurosphere cultures. After continued passaging, viability was lost in all Atr-deficient neurospheres.

not appear to have a primary role in p53-dependent signalling after DNA damage. Therefore, the sporadic apoptosis observed in $Atr^{Nes\text{-}cre}$ tissue likely results from replication-associated damage activating a DSB response via Atm-p53 signalling.

Defective neurogenesis in $Atr^{Nes\text{-}cre}$ mice does not require p53

DNA damage often results in either p53-dependent cell-cycle arrest or apoptosis, and both outcomes occur in the developing nervous system (Gao *et al*, 2000; Vousden and Lu, 2002; Orii *et al*, 2006; Lee and McKinnon, 2007). However, recently p53 loss was shown to exacerbate the effects of Atr deficiency because this abrogated two separate replication checkpoints (Murga *et al*, 2009; Ruzankina *et al*, 2009; Reaper *et al*, 2011). We therefore determined if p53 is relevant in neural Atr signalling by generating $Atr^{Nes\text{-}cre}$;$p53^{-/-}$ mice.

Histological analysis of $Atr^{Nes\text{-}cre}$;$p53^{-/-}$ mice showed very similar neuropathology to the $Atr^{Nes\text{-}cre}$ animals, indicating that in contrast to other scenarios (Murga *et al*, 2009; Ruzankina *et al*, 2009), p53 loss did not worsen the $Atr^{Nes\text{-}cre}$ phenotype (Figure 6A; Supplementary Figure S8). This can be seen by the similar cerebellar dysgenesis in the $Atr^{Nes\text{-}cre}$ and $Atr^{Nes\text{-}cre}$;$p53^{-/-}$ mice (Figure 6A). However, p53 loss resulted in attenuation of apoptosis in $Atr^{Nes\text{-}cre}$;$p53^{-/-}$ brains based upon TUNEL labelling in the GE and the EGL (Figure 6B and C). We also observed partial rescue of apoptosis in the $Atr^{Nes\text{-}cre}$ forebrain at later developmental stages (Figure 6B and D). The increased apoptosis in the developing $Atr^{Nes\text{-}cre}$ forebrain/cortex after E17.5 may result from accumulated DNA damage in cortical progenitors, and would explain the reduction of upper layer cortical neurons noted earlier (Figure 4E). However, despite reduced apoptosis in $Atr^{Nes\text{-}cre}$;$p53^{-/-}$ animals, only minimal amelioration of the $Atr^{Nes\text{-}cre}$ neuropathology was observed (Figure 6A). These data indicate that while p53 abrogates a portion of apoptosis resulting from Atr loss, it does not underpin the key features of the $Atr^{Nes\text{-}cre}$ phenotype such as cell-cycle arrest in the cerebellum.

We further examined the relationship between Atr and p53 using neurosphere cultures. We found that while either WT or $p53^{-/-}$ neurospheres readily established and grew robustly in culture, Atr-null cells failed to survive past 7 days in culture (Figure 6E). Despite this, we were able to initially establish cultures of $Atr^{Nes\text{-}cre}$ and $Atr^{Nes\text{-}cre}$;$p53^{-/-}$ neurospheres and observed a substantial enhancement of neurosphere size and growth in the $Atr^{Nes\text{-}cre}$;$p53^{-/-}$ cultures (Figure 6E, arrows). However, after 7 days in culture $Atr^{Nes\text{-}cre}$;$p53^{-/-}$ neurosphere expansion ceased and these cells failed to survive. These data indicate that the loss of p53 partially alleviates the consequences of Atr loss in neuroprogenitors, although these cells ultimately fail to survive.

Because p53 loss failed to ameliorate the effects of Atr inactivation, we also generated $(Atr;Ink4a/Arf)^{Nes\text{-}cre}$ mice to

determine the potential contribution of these cell-cycle regulators to the $Atr^{Nes\text{-}cre}$ phenotype. The *Ink4A/Arf* locus can be important for the maintenance of neural stem/progenitor cells and can influence their proliferation (Molofsky *et al*, 2006). However, we failed to see any phenotypic rescue or worsening of the $Atr^{Nes\text{-}cre}$ neural phenotype in $Atr;(Ink4a/Arf)^{Nes\text{-}cre}$ mice (Supplementary Figure S9). Thus, the pronounced neural phenotype resulting from Atr loss is not dependent upon signalling via either p53- or Ink4a/Arf-dependent cell-cycle arrest.

Atr functions independently from Atm during nervous system development

While loss of ATR or ATM leads to clinically distinct diseases (McKinnon, 2009), recent data support a close interrelationship between ATR and ATM in many settings, including the modulation of ATR by ATM during replication stress (Shechter *et al*, 2004; Jazayeri *et al*, 2006; Cuadrado *et al*, 2006a; Yoo *et al*, 2007; Shiotani and Zou, 2009b). Although ATM and ATR respond to different types of DNA damage, their many common substrates suggest potential overlapping biological functions (Matsuoka *et al*, 2007), and the potential compensatory function by one kinase in the absence of the other. However, interactions between ATR and ATM have not been fully explored physiologically, although germline inactivation of Atm in the setting of the $Atr^{S/S}$ Seckel syndrome model resulted in synthetic lethality (Murga *et al*, 2009). This outcome suggests critical functional redundancy between these two kinases. Therefore, we examined if these kinases cooperate *in vivo* in the developing nervous system.

We generated a conditional *Atm* allele that inactivated Atm via disruption of the kinase domain (Supplementary Figure S10). We found that embryonic inactivation of *Atm* by *Meox2-cre* produced a phenotype typical of $Atm^{-/-}$ tissue including the resistance of immature neural cells to DNA damage (Supplementary Figure S10) (Herzog *et al*, 1998; Lee *et al*, 2001). Therefore, using mice in which *Atm* and *Atr* were both conditionally inactivated, we determined if Atm signalling influenced the $Atr^{Nes\text{-}cre}$ phenotype. Mice lacking both Atm and Atr were viable and born at the expected ratio, and the gross appearance, weight and histological features of the brains of these mice were similar to $Atr^{Nes\text{-}cre}$ mice (Figure 7A and B). Calbindin immunostaining showed disruption of Purkinje cell patterning associated with defective granule cell genesis typical of $Atr^{Nes\text{-}cre}$ mice, which was unaffected by concomitant Atm deficiency (Figure 7A).

We further determined the relative levels of apoptosis and proliferation between $Atr^{Nes\text{-}cre};Atm^{Ctrl}$ and $(Atr;Atm)^{Nes\text{-}cre}$ animals at various embryonic stages. No histological differences were observed in the regions affected by Atr loss in the embryonic cerebellum or other areas in the $(Atr;Atm)^{Nes\text{-}cre}$ nervous system, when compared with age-matched $Atr^{Nes\text{-}cre};Atm^{Ctrl}$ embryos (data not shown).

As Atm activates apoptosis after DNA damage in immature postmitotic neurons (Herzog *et al*, 1998; Lee *et al*, 2001), we used TUNEL labelling to determine if apoptosis in the $Atr^{Nes\text{-}cre}$ GE and cerebellar EGL was Atm dependent and still occurred in $(Atr;Atm)^{Nes\text{-}cre}$ tissue. We found that in both regions, associated loss of Atm caused a significant decrease in the number of apoptotic cells (Figure 7C and D), although a fraction of these were dying via an Atm-independent manner. We also compared phosphorylation of p53ser18 between $Atr^{Nes\text{-}cre}Atm^{Ctrl}$ and $(Atr;Atm)^{Nes\text{-}cre}$ littermates and found that p53ser18 in the EGL of $Atr^{Nes\text{-}cre}Atm^{Ctrl}$ embryos was abrogated by Atm deficiency (Figure 7E). This suggests that the p53-positive cells observed in the embryonic EGL of $Atr^{Nes\text{-}cre}$ mice reflect granule precursor cells that acquired damage and initiate Atm-dependent apoptosis. Because coincident loss of Atm does not worsen the $Atr^{Nes\text{-}cre}$ phenotype, then the purported redundancy and direct functional cooperation between these kinases is equivocal, at least in the context of DNA processing during neural development. We also assessed the radiation response of the Atm and Atr double mutants, and found that p53 phosphorylation and TUNEL were Atm dependent and were not influenced by Atr status (Supplementary Figure S11). Thus, Atr and Atm function independently in the developing nervous system most likely in response to different DNA lesions, but may cooperate to ensure genomic stability.

Discussion

In this study, we investigated Atr function during mouse nervous system development. Understanding Atr function in this tissue is particularly relevant as human ATR-Seckel syndrome results in a profound neuropathology, as do a multitude of other human DNA repair deficiency diseases (McKinnon, 2009). Our data showed (1) an unexpected selectivity of ATR in monitoring certain progenitor populations during neurogenesis leading to a complex neural phenotype when its function is compromised, (2) that Atr- and p53-signalling interface differently in neural tissue to other organ systems and (3) that Atr and Atm fulfil different physiologic functions. In combination, these data highlight the tissue-specific roles for ATR in maintaining genome integrity, and illuminate pathology relevant to understanding ATR-Seckel syndrome.

We anticipated that neural Atr inactivation would broadly and substantially impact neurogenesis because germline deletion leads to a profound developmental defect (Brown and Baltimore, 2000; de Klein *et al*, 2000). Instead, we found that specific neural tissues such as the cerebellum and GE were markedly affected by Atr loss. However, in these cases, proliferation arrest underpins the $Atr^{Nes\text{-}cre}$ cerebellar phenotype while apoptosis occurs in the GE. Despite the different outcomes in these tissues after Atr loss, one common feature between these brain regions is their high relative proliferative index and continual cycling that generates large cohorts of progenitor cells. The rapid cycling of uncommitted progenitors likely increases replicative DNA damage that requires enhanced Atr-dependent genomic surveillance to ensure genomic integrity in subsequent progenitors. The requirement for Atr in these progenitors may be more stringent compared with the protracted cycles typical of differentiative divisions (Calegari *et al*, 2005; Dehay and Kennedy, 2007). This scenario is also consistent with the more severe cortical defects found in $Atr^{Emx1\text{-}cre}$ compared with $Atr^{Nes\text{-}cre}$. In that situation, *Emx1-cre* directs gene deletion to earlier progenitors that will subsequently undergo more division cycles in the absence of Atr than those from $Atr^{Nes\text{-}cre}$. These findings imply that Atr is critical for the long-term maintenance of rapidly proliferating progenitors, rather than individual cell cycles.

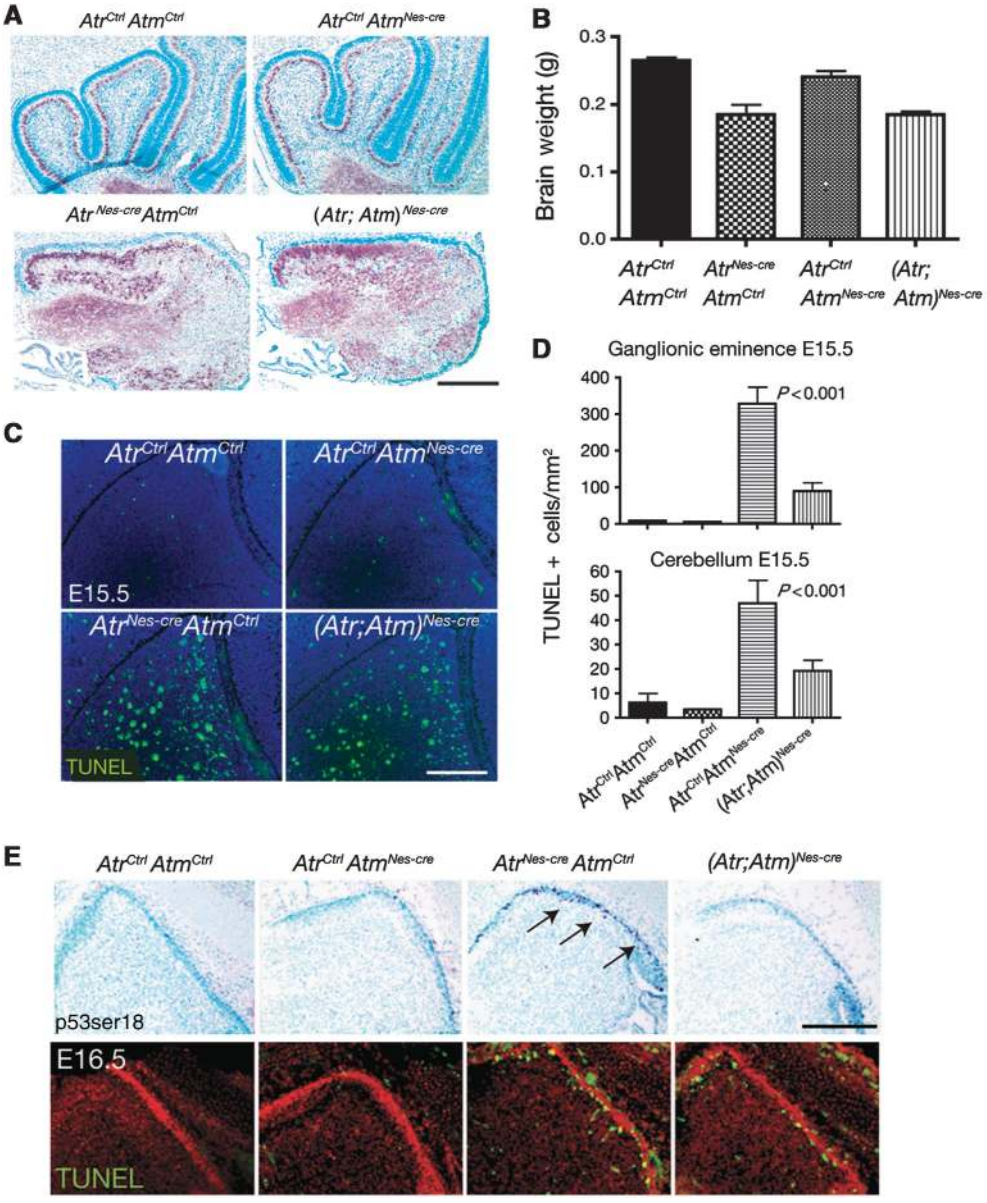

Figure 7 Coincident inactivation of Atm does not alter the $Atr^{Nes\text{-}cre}$ brain phenotype. (**A**) Mice at P5 in which both Atr and Atm were simultaneously deleted throughout the nervous system using *Nestin-cre* were similar to $Atr^{Nes\text{-}cre}$ mice with regard to histology and (**B**) overall brain weight. (**C**) As with the case for p53 loss, some apoptosis in the GE and cerebellum was Atm dependent. (**D**) Quantitation of cell death in the E15.5 GE and cerebellar EGL. (**E**) In the $Atr^{Nes\text{-}cre}$ cerebellum, p53ser18 phosphorylation is Atm dependent as is a fraction of apoptosis. All scale bars are ~300 μm.

The cerebellum was particularly affected by Atr loss. Initially, the $Atr^{Nes\text{-}cre}$ cerebellar anlage developed normally until around E15. At this stage, rapid proliferation of granule neurons occurs in the EGL in response to a pulse of the sonic hedgehog (Shh) mitogen. This presumably generates increased replication stress as GNPs rapidly expand and a concomitant enhanced need for vigilant genomic maintenance. Shh-driven expansion of the EGL is dependent upon GNP cilia, as a key Shh receptor, Patched-1, localizes to this organelle to modulate Shh signalling (Huangfu *et al*, 2003; Rohatgi *et al*, 2007). Disruption of cilia function, via inactivation of the Kif3a motor protein, leads to cerebellar defects similar to those seen in $Atr^{Nes\text{-}cre}$ cerebellum with a failure of EGL expansion around E16.5 (Chizhikov *et al*, 2007; Spassky *et al*, 2008; Han *et al*, 2009). Moreover, mice in which the Gli2 transcription factor has been inactivated also results in depletion of the EGL, as Gli2 activates Shh target genes (Corrales *et al*, 2004). While a functional ATR-Chk1 axis is important for activating cell-cycle checkpoints in response to replication fork abnormalities (Cimprich and Cortez, 2008; Lopez-Contreras and Fernandez-Capetillo, 2010), in our study, Atr loss results in granule neuron proliferation arrest. This indicates that replication-associated damage can result in ATR-independent proliferation arrest. As ATR activation depends upon TopBP1, deciphering the mammalian equivalents of other components of the active TopBP1 complex (e.g., Sld2, Sld3, Ticrr/TRESLIN and RHINO) will shed additional light upon DNA replication stress signalling and tissue development (Kumagai *et al*, 2010; Lopez-Mosqueda *et al*, 2010; Sansam *et al*, 2010; Zegerman and Diffley, 2010;

Cotta-Ramusino *et al*, 2011). Taken together, our data support a critical role for ATR in the cerebellum for monitoring replication-associated damage specifically during the Shh-driven rapid expansion of the EGL.

Cerebellar dysgenesis is part of the spectrum of neuropathology present in Seckel syndrome, while other characteristic neurological defects involve the CC, a large white matter structure that facilitates interhemispheric cross-talk (Shanske *et al*, 1997; Capovilla *et al*, 2001; Murga *et al*, 2009; Fitzgerald *et al*, 2011). Accordingly, we also found a marked defect in the CC after Atr inactivation, and this defect was more severe when Atr was deleted earlier in development using *Emx1-cre*. Pronounced effects of Atr loss were also found in the GE, a germinal centre for neural progenitors that migrate tangentially to areas throughout the telencephalon to generate a diversity of different cell types (Marin and Rubenstein, 2001; Flames *et al*, 2007; Fishell and Rudy, 2011). However, in contrast to the EGL, Atr loss results predominantly in apoptosis in this region rather than proliferation arrest. These alternate outcomes after DNA damage are not uncommon in the nervous system, and even within the cerebellum, a specific DNA repair defect such as Xrcc1 deficiency can lead to DNA damage-induced cell-cycle arrest in cerebellar interneurons but apoptosis in the EGL (Lee *et al*, 2009).

Recent studies found a detrimental synergistic effect of coincident loss of Atr and p53 likely from the combined effects of abolishment of independent cell-cycle checkpoints (Murga *et al*, 2009; Ruzankina *et al*, 2009; Reaper *et al*, 2011). This scenario may be further exacerbated by increased proliferation resulting from p53 loss (Gilad *et al*, 2010; Toledo *et al*, 2011). However, our study showed that in the nervous system, coincident loss of p53 and Atr did not result in additional defects above those in $Atr^{Nes\text{-}cre}$ tissue. This may reflect tissue specificity involving replication stress and p53 signalling. For example, different outcomes occur after Atm loss where in the small intestine and thymus many cell types are hypersensitive to IR-induced damage while immature neurons are resistant (Herzog *et al*, 1998; Lee *et al*, 2001). Combined deletion of Atm on the $Atr^{S/S}$ background resulted in lethality (Murga *et al*, 2009); although the basis for this is unclear, it probably does not relate to effects upon the nervous system. In our study, coordinate inactivation of Atm failed to exacerbate the $Atr^{Nes\text{-}cre}$ phenotype, suggesting that synthetic lethality in the scenario above resulted from effects in non-neural systems and at earlier stages of embryonic development.

Our data reveal a surprising plasticity in the neural progenitor requirement for Atr during development. In contrast to the inability of Atr-depleted cells to grow *in vitro*, neural progenitors lacking Atr can cycle. Depending upon the progenitor type, the consequences of Atr loss is variable, although proliferation is eventually compromised; perhaps as specific DNA lesions accumulate.

Materials and methods

Mice

The *Atr* floxed mice were as described (Ruzankina *et al*, 2007). *Nestin-Cre* and *Emx1-cre* mice were obtained from the Jackson Laboratory (B6.Cg-Tg(Nes-cre)1Kln/J; JAX #003771 and B6.129S2-$Emx1^{tm1(cre)Krj}$/J, JAX #005628). These were interbred in order to obtain $Atr^{LoxP/LoxP}$;*Nes-cre* mice. The control group (Atr^{Ctrl}) used was either $Atr^{LoxP/LoxP}$, $Atr^{+/LoxP}$;*Nes-cre* or $Atr^{+/+}$;*Nes-cre*. $Atm^{-/-}$ and $p53^{-/-}$ mice were as described (Herzog *et al*, 1998): these were interbred with $Atr^{LoxP/+}$;*Nes-cre* mice, and F1 mice were used to generate $Atr^{Nes\text{-}cre}$;$p53^{-/-}$ or $Atr^{Nes\text{-}cre}$;$Atm^{-/-}$. A *TopBP1* conditional allele was generated by flanking exons 3–6 with LoxP sites (manuscript in preparation). Floxed *Ink4a/Arf* mice were obtained from Professor Anton Berns (Netherlands Cancer Institute). An *Atm* conditional allele was generated in which LoxP sites flanked exon 58 (see Supplementary data). PCR to detect deletion of *Atr* used the following primers: ATR#10 (5′-CTATTTTTTGTTGCTGGTTTTG-3′) and ATR#15 (5′-CTTCTAATCTTCCTCCAGAATTGTAAAAGG-3′). Cre-TM mice (JAX #004682: B6.Cg-Tg(CAG-cre/Esr1)5Amc/J) provided tamoxifen-inducible cre expression driven from the actin promoter and were intercrossed with Atr^{LoxP} mice and used to obtain primary neural cell cultures.

Real-time PCR

Total DNA was extracted from tissues using the DNeasy Blood & Tissue Kit (Qiagen), according to the manufacturer's instructions. For real-time PCR analysis of *Atr* or *Atm* deletion in developing embryos, DNA was extracted from cryosections or frozen embryonic tissue at indicated ages. The measurement of *Atm* and *Atr* levels was done using aniQ SYBR Green Kit (Bio-Rad) with an iQ5 real-time PCR detection system (Bio-Rad). Gene deletion was determined using a ratio calculated from the targeted region to a common region of the gene using two different sets of PCR primers. For *Atr*, the targeted region (exon 44) used the forward primer 5′-GAAAGGAGCTTCGCCAGTGT and the reverse primer was 5′-GGGCAGGAGTAATTCTTGGAATAC; the common region (exon 29) was identified using the forward primer 5′-ACTCTGGCTGTAGCGTCCTTTC with the reverse primer 5′-TGCTTCTTTTCTGTAATAAATGACTCAAA. For the conditional *Atm* allele, the targeted region (exon 58) was detected using the forward primer 5′-TCAGCGAAGCGGTGTTCTC and the reverse primer 5′-TCATTTGGCCTGTATCTTCTATGTG. The common region (exon 52) was detected using the following primers: forward, 5′-ATGGAATGAAGATTTCATCCTATAAGTTT and the reverse primer was 5′-ATCCTAGGCCTCCCGTCATTT.

Histology

Mice were perfused with 4% (w/v) phosphate-buffered saline (PBS)-buffered paraformaldehyde (PFA) and cryoprotected in 25% PBS-buffered sucrose (w/v) solution. Brains were sectioned sagittally and sectioned at 10 μm using an HM500M cryostat (Microm). For analysis of paraffin-embedded tissue, mice were perfused with PFA and 5 μm sections were dewaxed in xylene prior to staining. Nissl staining was carried out with 1% (w/v) thionin. Haematoxylin and eosin staining was done according to the standard procedures. Immunohistochemical staining of tissues was carried out with the antibodies listed below. For colorimetric visualization of positive signals, sections were incubated with antibodies overnight at room temperature after quenching endogenous peroxidase using 0.6% (v/v) H_2O_2 in methanol. Slides were washed with PBS three times, followed by incubation with biotinylated secondary antibody and avidin–biotin complex (Vectastain Elite kit, Vector Labs). Antibodies were used after citrate buffer-based antigen retrieval. Immunoreactivity was visualized with the VIP substrate kit (Vector Labs) using the manufacturer's protocol. After staining, sections were counterstained with 0.1% (w/v) methyl green, dehydrated,and mounted in DPX (Fluka). For fluorescent signals of immunoreactivity, FITC- or Cy3-conjugated secondary antibodies (Jackson Immunologicals) were used and counterstained with 4′6-diamidino-2-phenylindole (DAPI) or propidium iodide (Vector Laboratories). The following antibodies were used: anti-calbindin (mouse, 1:2000; Sigma), anti-PCNA (mouse, 1:500; Santa Cruz Biotechnology), Pax2 (rabbit, 1:500; Zymed), Ki67 (rabbit, 1:250; Vector Laboratories), anti-BrdU (rat, 1/500; Oxford Biotechnology), anti-active Caspase-3 (1/100; BD Biosciences), anti-p53ser15 (rabbit, 1/100; Cell Signaling), anti-pH2AXser139 (rabbit, 1/500; Abcam), anti-pH3ser10 (rabbit, 1/500; Cell Signaling), anti-Cux1 (CDP, rabbit, 1:100; Santa Cruz Biotechnology), anti-Brn2 (rabbit, 1:200; GeneTex), anti-Satb2 (mouse, 1:50; Abcam), anti-Tbr1 (rabbit, 1:100; Abcam), anti-Ctip2 (rat, 1:100; Abcam), anti-Tbr2 (rabbit, 1:200; Abcam), anti-Foxp1 (mouse, 1:50; Thermo Fisher Scientific), and anti-Foxp2 (rabbit, 1:50; Abnova). For *in vivo* proliferation assays, newborn mice or pregnant females were injected intraperitonally with BrdU at 50 μg/g of body weight (Sigma-Aldrich). The embryos or brains were removed either 2 or 6 h after injection and fixed in 4% PBS-buffered PFA. TUNEL

analysis was performed using cryosections with the ApopTag® fluorescein *In situ* Apoptosis Detection Kit (Chemicon) according to the manufacturer's directions.

Cell counts

Quantification of specific cell populations were used to determine indices of cell cycle or apoptosis during embryonic brain development in Atr conditional animals. Three embryos were analysed per each time point and for each genotype. Immunopositive signals for PCNA, pH3ser10 and BrdU within 1 mm^2 were measured from at least three representative sections per each embryo. For the forebrain and GE, cells were assessed in a 0.27 mm^2 area for PCNA and BrdU-positive cells; forebrain refers to the neopallial cortex. Midbrain is the area directly above the cerebellum (future colliculus); the developing cerebellum and was divided into three areas, the VZ, LR and EGL. All data and statistics were done using Prism (v4.0, Graphpad); $P<0.05$ was considered as significant.

Western blots

Western blot analysis was performed with tissues (cortex, cerebella, liver and spleen) from both P5 control mice ($Atr^{LoxP/+}$;*Nes-cre or* $Atr^{LoxP/LoxP}$) and conditional knockout mice ($Atr^{Nes\text{-}cre}$, $Atr^{Emx1\text{-}cre}$ and $TopBP1^{Nes\text{-}cre}$). Protein extracts were prepared by using lysis buffer (50 mM Tris–HCl, 200 mM NaCl, 0.2% NP-40, 1% Tween-20 (v/v), 1 mM NaF, 1 mM sodium vanadate, 50 mM β-glycerophosphate, 2 mM PMSF, and protease inhibitor cocktail (Roche)) and quantified by Bradford assay (Bio-Rad). Proteins (50μg per lane) were separated through a 4–12% (w/v) Bis-Tris SDS polyacrylamide gel (Invitrogen) and transferred onto nitrocellulose membrane (Bio-Rad). Blots were sequentially immunostained with anti-ATR (goat, 1:130; Santa Cruz), anti-TopBP1 antibody (rabbit, 1:1000; Chemicon) followed by horseradish peroxidase-conjugated secondary antibodies (1:1000; GE Healthcare) and detected using ECL Plus chemiluminescence reagent (GE Healthcare). Blots were also probed with anti-Nbs1 (rabbit, 1:500; Cell Signaling), anti-Chk2 (mouse, 1:1000; Millipore), anti-p53ser15 (rabbit, 1/1000; Cell Signaling), anti-pChk1ser317 (rabbit, 1/800; Bethyl) and processed as described above. Ponceau staining and anti-actin immunoblotting (goat, 1:500; Santa Cruz Biotech) of the transferred membrane were used as protein-loading controls.

Isolation and analysis of primary astrocytes

Primary astrocytes were prepared from control or $Atr^{Nes\text{-}cre}$;$p53^{-/-}$ P1 mouse brains. Cortices were dissociated by passage through a 5-ml pipette and cells were resuspended in Dulbecco's modified Eagle's medium and Ham's nutrient mixture F12 (1:1 DMEM/F12; Gibco-BRL) supplemented with 10% fetal bovine serum (v/v), 100 U/ml penicillin, 100 μg/ml streptomycin and 20 ng/ml epidermal growth factor (Millipore). Primary astrocytes were established in Primeria T-25 tissue culture flasks (Falcon) at 37°C in a humidified 5% CO_2 incubator. After 4 days, cells were trypsinized and seeded onto round 1 mm glass coverslips in 24-well plates. Cells were allowed to re-establish for 24 h followed by fixation in 4% PFA and permeabilization in PBS-buffered 0.5% Triton X-100. Cells were subsequently incubated with anti-GFAP (mouse, 1:500; Sigma) and anti-γH2AX (rabbit, 1:500; Millipore) antibodies for 1 h at room temperature, washed and labelled with anti-mouse Alexa 488-conjugated and anti-rabbit Alexa 555-conjugated antibodies (Invitrogen). Cells were mounted and counterstained with Vectastain/DAPI (Vector Laboratories) and visualized.

Neurosphere cultures

Neurospheres were isolated from finely minced neocortex of E13.5 embryos. A digestion solution of 300 μl DMEM–F12 with glutamax, penicillin and streptomycin, papain (30 U/ml), cysteine (0.24 mg/ml) and DNAse1 (0.4 mg/ml) was added to the dissociated tissue and incubated 37°C for 45 min, inverting several times during incubation. Digestion was stopped by addition of 300 μl inhibitor solution (L15 medium, ovomucoid trypsin inhibitor (1.125 mg/ml) BSA (0.5 mg/ml), DNAse1 (4 mg/ml)) incubated for 5 min 37°C and another 300 μl inhibitor solution was added. The tissue was passed through a Pasteur pipet $\times 10$ followed by $\times 4$ through a $27^{1/2}$ gauge needle and washed in media. Neurospheres were maintained using NeuroCult NSC basal media (Stemcell Technologies) supplemented with NeuroCult NSC proliferation supplement and 20 ng/ml recombinant human EGF. Cultures in T25 flasks were incubated for 2 h to remove MEFs and gently agitated daily to prevent clumping of neurospheres. After 3–4 days, 1 ml of NeuroCult NSC basal media was added and the cells passaged at day 7. Real-time PCR analysis was used to measure deletion efficiency of *Atr* exon 44 after tamoxifen induction and deletion was >90%. Cells were treated with 1 μM 4OHT (Sigma) for 48 h. ATM inhibitor (KU55933; Sigma) at 1 μM or DNA-PK_{CS} inhibitor (NU7026; Sigma) at 5 μM was added 1 h prior to irradiation.

Supplementary data

Supplementary data are available at *The EMBO Journal* Online (http://www.embojournal.org).

Acknowledgements

We thank the Hartwell Center for biotech support, the Transgenic core facility for blastocyst injections and the ARC for animal husbandry. PJM was supported by the NIH (NS-37956, CA-21765), the CCSG (P30 CA21765) and the American Lebanese and Syrian Associated Charities of St Jude Children's Research Hospital. SK is a Neoma Boadway AP Endowed Fellow. EJB was supported by the NIH (AG-027376 and an ARRA supplement).

Author contribution: YL, ERPS, P-OF, SK, VE-R and HRR performed all the experiments characterizing the murine models of ATR-deficiency mouse and contributed to writing the manuscript. ERPS and HRR generated Atm conditional mutant mice. JZ generated western blot data. JZ and HRR were responsible for mouse colony production and maintenance. EJB provided Atr-deficient mice and contributed to the final version of the manuscript. PJM was project leader and produced the final version of the manuscript.

Conflict of interest

The authors declare that they have no conflict of interest.

References

Branzei D, Foiani M (2010) Maintaining genome stability at the replication fork. *Nat Rev Mol Cell Biol* **11:** 208–219

Brown EJ, Baltimore D (2000) ATR disruption leads to chromosomal fragmentation and early embryonic lethality. *Genes Dev* **14:** 397–402

Calegari F, Haubensak W, Haffner C, Huttner WB (2005) Selective lengthening of the cell cycle in the neurogenic subpopulation of neural progenitor cells during mouse brain development. *J Neurosci* **25:** 6533–6538

Capovilla G, Lorenzetti ME, Montagnini A, Borgatti R, Piccinelli P, Giordano L, Accorsi P, Caudana R (2001) Seckel's syndrome and malformations of cortical development: report of three new cases and review of the literature. *J Child Neurol* **16:** 382–386

Chini CC, Chen J (2003) Human claspin is required for replication checkpoint control. *J Biol Chem* **278:** 30057–30062

Chizhikov VV, Davenport J, Zhang Q, Shih EK, Cabello OA, Fuchs JL, Yoder BK, Millen KJ (2007) Cilia proteins control cerebellar morphogenesis by promoting expansion of the granule progenitor pool. *J Neurosci* **27:** 9780–9789

Chou SJ, Perez-Garcia CG, Kroll TT, O'Leary DD (2009) Lhx2 specifies regional fate in Emx1 lineage of telencephalic progenitors generating cerebral cortex. *Nat Neurosci* **12:** 1381–1389

Chun HH, Gatti RA (2004) Ataxia-telangiectasia, an evolving phenotype. *DNA Repair* **3:** 1187–1196

Cimprich KA, Cortez D (2008) ATR: an essential regulator of genome integrity. *Nat Rev Mol Cell Biol* **9:** 616–627

Corbin JG, Nery S, Fishell G (2001) Telencephalic cells take a tangent: non-radial migration in the mammalian forebrain. *Nat Neurosci* **4**(Suppl)**:** 1177–1182

Corrales JD, Rocco GL, Blaess S, Guo Q, Joyner AL (2004) Spatial pattern of sonic hedgehog signaling through Gli genes during cerebellum development. *Development* **131:** 5581–5590

Cortez D, Guntuku S, Qin J, Elledge SJ (2001) ATR and ATRIP: partners in checkpoint signaling. *Science* **294:** 1713–1716

Cotta-Ramusino C, McDonald III ER, Hurov K, Sowa ME, Harper JW, Elledge SJ (2011) A DNA damage response screen identifies RHINO, a 9-1-1 and TopBP1 interacting protein required for ATR signaling. *Science* **332:** 1313–1317

Cuadrado M, Martinez-Pastor B, Fernandez-Capetillo O (2006a) ATR activation in response to ionizing radiation: still ATM territory. *Cell Division* **1:** 7

Cuadrado M, Martinez-Pastor B, Murga M, Toledo LI, Gutierrez-Martinez P, Lopez E, Fernandez-Capetillo O (2006b) ATM regulates ATR chromatin loading in response to DNA double-strand breaks. *J Exp Med* **203:** 297–303

Dehay C, Kennedy H (2007) Cell-cycle control and cortical development. *Nat Rev Neurosci* **8:** 438–450

de Klein A, Muijtjens M, van Os R, Verhoeven Y, Smit B, Carr AM, Lehmann AR, Hoeijmakers JH (2000) Targeted disruption of the cell-cycle checkpoint gene ATR leads to early embryonic lethality in mice. *Curr Biol* **10:** 479–482

Delacroix S, Wagner JM, Kobayashi M, Yamamoto K, Karnitz LM (2007) The Rad9-Hus1-Rad1 (9-1-1) clamp activates checkpoint signaling via TopBP1. *Genes Dev* **21:** 1472–1477

Fishell G, Rudy B (2011) Mechanisms of inhibition within the telencephalon: ''Where the Wild Things Are''. *Annu Rev Neurosci* **34:** 535–567

Fitzgerald B, O'Driscoll M, Chong K, Keating S, Shannon P (2011) Neuropathology of fetal stage Seckel syndrome: a case report providing a morphological correlate for the emerging molecular mechanisms. *Brain Dev* (advance online publication, 11 Jun 2011)

Flames N, Pla R, Gelman DM, Rubenstein JL, Puelles L, Marin O (2007) Delineation of multiple subpallial progenitor domains by the combinatorial expression of transcriptional codes. *J Neurosci* **27:** 9682–9695

Gao Y, Ferguson DO, Xie W, Manis JP, Sekiguchi J, Frank KM, Chaudhuri J, Horner J, DePinho RA, Alt FW (2000) Interplay of p53 and DNA-repair protein XRCC4 in tumorigenesis, genomic stability and development. *Nature* **404:** 897–900

Gilad O, Nabet BY, Ragland RL, Schoppy DW, Smith KD, Durham AC, Brown EJ (2010) Combining ATR suppression with oncogenic Ras synergistically increases genomic instability, causing synthetic lethality or tumorigenesis in a dosage-dependent manner. *Cancer Res* **70:** 9693–9702

Gorski JA, Talley T, Qiu M, Puelles L, Rubenstein JL, Jones KR (2002) Cortical excitatory neurons and glia, but not GABAergic neurons, are produced in the Emx1-expressing lineage. *J Neurosci* **22:** 6309–6314

Han YG, Kim HJ, Dlugosz AA, Ellison DW, Gilbertson RJ, Alvarez-Buylla A (2009) Dual and opposing roles of primary cilia in medulloblastoma development. *Nat Med* **15:** 1062–1065

Herzog KH, Chong MJ, Kapsetaki M, Morgan JI, McKinnon PJ (1998) Requirement for Atm in ionizing radiation-induced cell death in the developing central nervous system. *Science* **280:** 1089–1091

Hisaoka T, Nakamura Y, Senba E, Morikawa Y (2010) The forkhead transcription factors, Foxp1 and Foxp2, identify different subpopulations of projection neurons in the mouse cerebral cortex. *Neuroscience* **166:** 551–563

Hopfner KP, Craig L, Moncalian G, Zinkel RA, Usui T, Owen BA, Karcher A, Henderson B, Bodmer JL, McMurray CT, Carney JP, Petrini JH, Tainer JA (2002) The Rad50 zinc-hook is a structure joining Mre11 complexes in DNA recombination and repair. *Nature* **418:** 562–566

Huangfu D, Liu A, Rakeman AS, Murcia NS, Niswander L, Anderson KV (2003) Hedgehog signalling in the mouse requires intraflagellar transport proteins. *Nature* **426:** 83–87

Jackson SP, Bartek J (2009) The DNA-damage response in human biology and disease. *Nature* **461:** 1071–1078

Jazayeri A, Falck J, Lukas C, Bartek J, Smith GC, Lukas J, Jackson SP (2006) ATM- and cell cycle-dependent regulation of ATR in response to DNA double-strand breaks. *Nat Cell Biol* **8:** 37–45

Kumagai A, Dunphy WG (2003) Repeated phosphopeptide motifs in Claspin mediate the regulated binding of Chk1. *Nat Cell Biol* **5:** 161–165

Kumagai A, Lee J, Yoo HY, Dunphy WG (2006) TopBP1 activates the ATR-ATRIP complex. *Cell* **124:** 943–955

Kumagai A, Shevchenko A, Dunphy WG (2010) Treslin collaborates with TopBP1 in triggering the initiation of DNA replication. *Cell* **140:** 349–359

Lavdas AA, Grigoriou M, Pachnis V, Parnavelas JG (1999) The medial ganglionic eminence gives rise to a population of early neurons in the developing cerebral cortex. *J Neurosci* **19:** 7881–7888

Lavin MF (2008) Ataxia-telangiectasia: from a rare disorder to a paradigm for cell signalling and cancer. *Nat Rev Mol Cell Biol* **9:** 759–769

Lee J, Kumagai A, Dunphy WG (2003) Claspin, a Chk1-regulatory protein, monitors DNA replication on chromatin independently of RPA, ATR, and Rad17. *Mol Cell* **11:** 329–340

Lee J, Kumagai A, Dunphy WG (2007) The Rad9-Hus1-Rad1 checkpoint clamp regulates interaction of TopBP1 with ATR. *J Biol Chem* **282:** 28036–28044

Lee Y, Chong MJ, McKinnon PJ (2001) Ataxia telangiectasia mutated-dependent apoptosis after genotoxic stress in the developing nervous system is determined by cellular differentiation status. *J Neurosci* **21:** 6687–6693

Lee Y, Katyal S, Li Y, El-Khamisy SF, Russell HR, Caldecott KW, McKinnon PJ (2009) The genesis of cerebellar interneurons and the prevention of neural DNA damage require XRCC1. *Nat Neurosci* **12:** 973–980

Lee Y, McKinnon PJ (2007) Responding to DNA double strand breaks in the nervous system. *Neuroscience* **145:** 1365–1374

Limbo O, Porter-Goff ME, Rhind N, Russell P (2011) Mre11 nuclease activity and Ctp1 regulate Chk1 activation by Rad3ATR and Tel1ATM checkpoint kinases at double-strand breaks. *Mol Cell Biol* **31:** 573–583

Liu Q, Guntuku S, Cui XS, Matsuoka S, Cortez D, Tamai K, Luo G, Carattini-Rivera S, DeMayo F, Bradley A, Donehower LA, Elledge SJ (2000) Chk1 is an essential kinase that is regulated by Atr and required for the G(2)/M DNA damage checkpoint. *Genes Dev* **14:** 1448–1459

Lopez-Contreras AJ, Fernandez-Capetillo O (2010) The ATR barrier to replication-born DNA damage. *DNA Repair* **9:** 1249–1255

Lopez-Mosqueda J, Maas NL, Jonsson ZO, Defazio-Eli LG, Wohlschlegel J, Toczyski DP (2010) Damage-induced phosphorylation of Sld3 is important to block late origin firing. *Nature* **467:** 479–483

Marin O, Rubenstein JL (2001) A long, remarkable journey: tangential migration in the telencephalon. *Nat Rev Neurosci* **2:** 780–790

Matsuoka S, Ballif BA, Smogorzewska A, McDonald III ER, Hurov KE, Luo J, Bakalarski CE, Zhao Z, Solimini N, Lerenthal Y, Shiloh Y, Gygi SP, Elledge SJ (2007) ATM and ATR substrate analysis reveals extensive protein networks responsive to DNA damage. *Science* **316:** 1160–1166

McKinnon PJ (2009) DNA repair deficiency and neurological disease. *Nat Rev Neurosci* **10:** 100–112

McKinnon PJ (2012) ATM and the molecular pathogenesis of ataxia telangiectasia. *Annu Rev Pathol* **7:** 303–321

Molofsky AV, Slutsky SG, Joseph NM, He S, Pardal R, Krishnamurthy J, Sharpless NE, Morrison SJ (2006) Increasing p16INK4a expression decreases forebrain progenitors and neurogenesis during ageing. *Nature* **443:** 448–452

Molyneaux BJ, Arlotta P, Menezes JR, Macklis JD (2007) Neuronal subtype specification in the cerebral cortex. *Nat Rev Neurosci* **8:** 427–437

Mordes DA, Glick GG, Zhao R, Cortez D (2008) TopBP1 activates ATR through ATRIP and a PIKK regulatory domain. *Genes Dev* **22:** 1478–1489

Moreno-Herrero F, de Jager M, Dekker NH, Kanaar R, Wyman C, Dekker C (2005) Mesoscale conformational changes in the DNA-repair complex Rad50/Mre11/Nbs1 upon binding DNA. *Nature* **437:** 440–443

Murga M, Bunting S, Montana MF, Soria R, Mulero F, Canamero M, Lee Y, McKinnon PJ, Nussenzweig A, Fernandez-Capetillo O (2009) A mouse model of ATR-Seckel shows embryonic replicative stress and accelerated aging. *Nat Genet* **41:** 891–898

Nam EA, Cortez D (2011) ATR signalling: more than meeting at the fork. *Biochem J* **436:** 527–536

O'Driscoll M, Ruiz-Perez VL, Woods CG, Jeggo PA, Goodship JA (2003) A splicing mutation affecting expression of ataxia-telangiectasia and Rad3-related protein (ATR) results in Seckel syndrome. *Nat Genet* **33:** 497–501

Ohouo PY, Bastos de Oliveira FM, Almeida BS, Smolka MB (2010) DNA damage signaling recruits the Rtt107-Slx4 scaffolds via Dpb11 to mediate replication stress response. *Mol Cell* **39:** 300–306

Onksen JL, Brown EJ, Blendy JA (2011) Selective deletion of a cell cycle checkpoint kinase (ATR) reduces neurogenesis and alters responses in rodent models of behavioral affect. *Neuropsychopharmacology* **36:** 960–969

Orii KE, Lee Y, Kondo N, McKinnon PJ (2006) Selective utilization of nonhomologous end-joining and homologous recombination DNA repair pathways during nervous system development. *Proc Natl Acad Sci USA* **103:** 10017–10022

Reaper PM, Griffiths MR, Long JM, Charrier JD, Maccormick S, Charlton PA, Golec JM, Pollard JR (2011) Selective killing of ATM- or p53-deficient cancer cells through inhibition of ATR. *Nat Chem Biol* **7:** 428–430

Rohatgi R, Milenkovic L, Scott MP (2007) Patched1 regulates hedgehog signaling at the primary cilium. *Science* **317:** 372–376

Rouse J (2004) Esc4p, a new target of Mec1p (ATR), promotes resumption of DNA synthesis after DNA damage. *EMBO J* **23:** 1188–1197

Rudy B, Fishell G, Lee S, Hjerling-Leffler J (2011) Three groups of interneurons account for nearly 100% of neocortical GABAergic neurons. *Dev Neurobiol* **71:** 45–61

Ruzankina Y, Pinzon-Guzman C, Asare A, Ong T, Pontano L, Cotsarelis G, Zediak VP, Velez M, Bhandoola A, Brown EJ (2007) Deletion of the developmentally essential gene ATR in adult mice leads to age-related phenotypes and stem cell loss. *Cell Stem Cell* **1:** 113–126

Ruzankina Y, Schoppy DW, Asare A, Clark CE, Vonderheide RH, Brown EJ (2009) Tissue regenerative delays and synthetic lethality in adult mice after combined deletion of Atr and Trp53. *Nat Genet* **41:** 1144–1149

Sansam CL, Cruz NM, Danielian PS, Amsterdam A, Lau ML, Hopkins N, Lees JA (2010) A vertebrate gene, ticrr, is an essential checkpoint and replication regulator. *Genes Dev* **24:** 183–194

Sar F, Lindsey-Boltz LA, Subramanian D, Croteau DL, Hutsell SQ, Griffith JD, Sancar A (2004) Human claspin is a ring-shaped DNA-binding protein with high affinity to branched DNA structures. *J Biol Chem* **279:** 39289–39295

Shanske A, Caride DG, Menasse-Palmer L, Bogdanow A, Marion RW (1997) Central nervous system anomalies in Seckel syndrome: report of a new family and review of the literature. *Am J Med Genet* **70:** 155–158

Shechter D, Costanzo V, Gautier J (2004) ATR and ATM regulate the timing of DNA replication origin firing. *Nat Cell Biol* **6:** 648–655

Shiloh Y (2006) The ATM-mediated DNA-damage response: taking shape. *Trends Biochem Sci* **31:** 402–410

Shiotani B, Zou L (2009a) ATR signaling at a glance. *J Cell Sci* **122:** 301–304

Shiotani B, Zou L (2009b) Single-stranded DNA orchestrates an ATM-to-ATR switch at DNA breaks. *Mol Cell* **33:** 547–558

Sohn SY, Cho Y (2009) Crystal structure of the human rad9-hus1-rad1 clamp. *J Mol Biol* **390:** 490–502

Spassky N, Han YG, Aguilar A, Strehl L, Besse L, Laclef C, Ros MR, Garcia-Verdugo JM, Alvarez-Buylla A (2008) Primary cilia are required for cerebellar development and Shh-dependent expansion of progenitor pool. *Dev Biol* **317:** 246–259

Stracker TH, Theunissen JW, Morales M, Petrini JH (2004) The Mre11 complex and the metabolism of chromosome breaks: the importance of communicating and holding things together. *DNA Repair (Amst)* **3:** 845–854

Suh H, Consiglio A, Ray J, Sawai T, D'Amour KA, Gage FH (2007) *In vivo* fate analysis reveals the multipotent and self-renewal capacities of Sox2 + neural stem cells in the adult hippocampus. *Cell Stem Cell* **1:** 515–528

Toledo LI, Murga M, Zur R, Soria R, Rodriguez A, Martinez S, Oyarzabal J, Pastor J, Bischoff JR, Fernandez-Capetillo O (2011) A cell-based screen identifies ATR inhibitors with synthetic lethal properties for cancer-associated mutations. *Nat Struct Mol Biol* **18:** 721–727

Tomimatsu N, Mukherjee B, Burma S (2009) Distinct roles of ATR and DNA-PKcs in triggering DNA damage responses in ATM-deficient cells. *EMBO Rep* **10:** 629–635

Vousden KH, Lu X (2002) Live or let die: the cell's response to p53. *Nat Rev Cancer* **2:** 594–604

Xu X, Vaithiyalingam S, Glick GG, Mordes DA, Chazin WJ, Cortez D (2008) The basic cleft of RPA70N binds multiple checkpoint proteins, including RAD9, to regulate ATR signaling. *Mol Cell Biol* **28:** 7345–7353

Yoo HY, Kumagai A, Shevchenko A, Dunphy WG (2009) The Mre11-Rad50-Nbs1 complex mediates activation of TopBP1 by ATM. *Mol Biol Cell* **20:** 2351–2360

Yoo HY, Kumagai A, Shevchenko A, Shevchenko A, Dunphy WG (2007) Ataxia-telangiectasia mutated (ATM)-dependent activation of ATR occurs through phosphorylation of TopBP1 by ATM. *J Biol Chem* **282:** 17501–17506

Zappone MV, Galli R, Catena R, Meani N, De Biasi S, Mattei E, Tiveron C, Vescovi AL, Lovell-Badge R, Ottolenghi S, Nicolis SK (2000) Sox2 regulatory sequences direct expression of a (beta)-geo transgene to telencephalic neural stem cells and precursors of the mouse embryo, revealing regionalization of gene expression in CNS stem cells. *Development* **127:** 2367–2382

Zegerman P, Diffley JF (2010) Checkpoint-dependent inhibition of DNA replication initiation by Sld3 and Dbf4 phosphorylation. *Nature* **467:** 474–478

Zhao H, Piwnica-Worms H (2001) ATR-mediated checkpoint pathways regulate phosphorylation and activation of human Chk1. *Mol Cell Biol* **21:** 4129–4139

Zou L, Elledge SJ (2003) Sensing DNA damage through ATRIP recognition of RPA-ssDNA complexes. *Science* **300:** 1542–1548